Publikationen des Deutschen Archäologischen Instituts

Wolfgang Rabbel, Ercan Erkul, Rebekka Mecking, Harald Stümpel

Geophysical Prospection of Monumental Burial Mounds

in: Pirson et al. - Hellenistic Funerary Culture in Pergamon and the Aeolis: A Collection of Current Approaches and New Results

https://doi.org/10.34780/0nbear21

Herausgebende Institution / Publisher:
Deutsches Archäologisches Institut

Geophysical Prospection of Monumental Burial Mounds

Wolfgang Rabbel – Ercan Erkul – Rebekka Mecking – Harald Stümpel

1. Introduction

Since the Neolithic, burial mounds have been a major formative element of ancient land- and cityscapes. In their construction they show high variability making classifications often difficult, even within selected epochs and regions. This applies especially to the tumuli of the Hellenistic Eastern Mediterranean and their monumental predecessors[1]. While their height usually ranges from a few metres to tens of metres, in this region burial mounds reach up to 50 m in height and 150 m in diameter at the base. However, the size and depth of a possible interior funeral construction, or even the presence of one, is mostly unknown.

The archaeological investigation of monumental tumuli is a challenging task in many respects. The sheer size of the mounds restricts excavations usually to the near-surface – unless the destruction of the monument is condoned. The lack of regularity of internal construction makes conclusions by analogy with other mounds highly uncertain, almost speculative. Even geophysical sounding is challenging because metre-scale archaeological objects are to be located possibly at a depth of tens of metres, which causes a significant resolution and range problem for most sounding methods.

Indeed, few examples of geophysical investigations of large grave mounds have been reported in the literature[2]. Typically, electric resistivity tomography or seismic refraction tomography were applied to investigate the deepest parts of the mounds, both methods suffering from severe losses of resolution at increasing depths. Therefore, we intend to direct attention to seismic reflection imaging as an alternative prospection method, which has been applied only rarely in archaeological contexts. For tumuli exploration it was applied for the first time in the pioneering study of Lütjen and Utecht at Nemrud Dağ[3].

Against this background, the objectives of the present article are (1) to concretely identify which sort of tumuli-related archaeological targets can be explored by which geophysical means, (2) to outline a corresponding prospection concept considering the given geological frame, and (3) to illustrate it using results from the Yığma Tepe case-study of Pergamon. Regarding the prospection concept, the article takes a general perspective that can be applied to other sites as well.

Prospection goals achievable by geophysical sounding and a corresponding prospection concept are outlined in section 2 while examples from Yığma Tepe are shown in section 3[4].

1 Many examples can be found, e. g., in: Henry – Kelp 2016.
2 Goell 1969; Lütjen – Utecht 1991; Polymenakos – Tweeton 2015; Polymenakos – Tweeton 2017; Tsokas et al. 2018.
3 Lütjen – Utecht 1991.
4 More results from Yığma Tepe can be found in the article of Meinecke et al. in this volume.

DOI: https://doi.org/10.34780/0nbear21

2. Developing a Prospection Concept

2.1. Mound-Related Prospection Targets

Monumental grave mounds have to be regarded as being potentially multi-phased in both construction and use over the millennia. Accordingly, three major groups of investigation targets may be distinguished, each requiring different prospection approaches:

1. *Grave chambers and dromoi* are usually the primary targets of archaeological interest. They may be found at any depth within grave mounds, even below the base level. In the case of Yığma Tepe this means that depths of up to 40 m need to be investigated, which exceeds the sounding range of the methods commonly applied in archaeological prospecting. Chamber diameters are on the order of only a few metres, which is small in comparison to the possible depth location. These circumstances imply that applicable prospecting methods need to combine a metre-scale spatial resolution with higher than usual sounding depth.
2. *Stratigraphy*: The layering of mounds can be examined in terms of changes in the physical parameters of the piled-up soils or rocks. This geophysical stratigraphy provides information on the overbuilt base relief, the depths and shapes of different construction phases, levels of changing soil compaction, and moisture penetration – information helpful to understand the construction and evolution of the mound as a whole.
3. *Near-surface archaeological targets* may be multiform and strongly variable in age. They may include remains of ornamental or ritual architecture such as enclosing walls or monument foundations, constructional elements such as supporting walls or ramps, secondary burials, or other forms of secondary usage, for instance agricultural.

2.2. Geophysical Prospection Methods Reviewed

Recent investigations of burial mounds have relied on combining different geophysical methods, mostly ground penetrating radar (GPR), electric resistivity tomography (ERT) and magnetics. This approach was shown to be successful for ›small‹ – meaning a few metres high – burial mounds[5]. However, it fails for larger mounds because of a number of reasons: Except in very dry pure sands, GPR penetration depth is limited to only a few metres depending on the clay and moisture content of the soil; ERT measurements[6] can easily penetrate 10 m and more, but the tomographic resolution is only on the same order as the penetration depth; and magnetic anomalies have no reliable depth resolution and decay rapidly with the depth of the magnetic source. At the Earth's surface the magnetic signals of deep burial chambers would be weak, smeared out in an area with a diameter relative to the source depth and would have interference from the geological background signal.

To demonstrate this, we numerically compute the physical effects of a grave chamber and their dependence on the chamber depth for the geophysical methods commonly applied in archaeological prospecting. In all cases the chamber is approximated by a spherical cavity. The resulting signal strengths can then be compared to the theoretical and practical detection limits of the respective field instruments (figs. 1. 2). The underlying model assumptions and

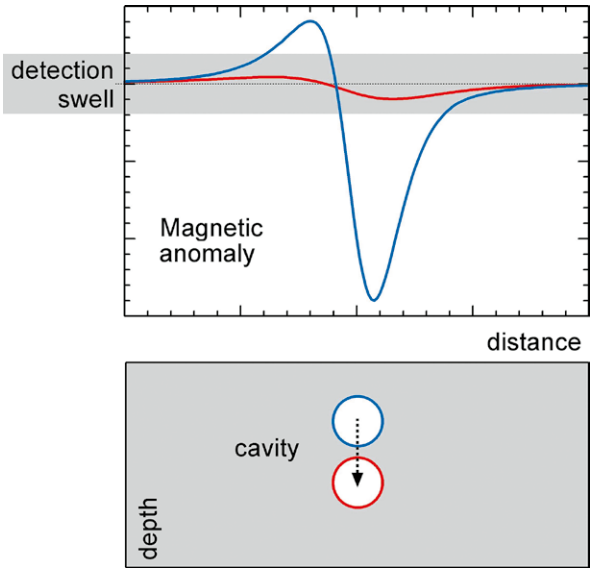

1 Change of the magnetic anomaly of a cavity with increasing cavity depth as an example for a detection swell (cf. blue vs. red graph). The detection swell is shown as a grey bar in the top figure. It defines the minimum size the magnetic signal of a target in order to be identifiable

5 E. g. Persson – Olofsson 2004; Tonkov – Loke 2006.

6 E. g. Tonkov 1996.

formulae are explained in detail in the Appendix. In the following sections 2.2.1 to 2.2.4 the results are summarised and illustrated. The outcome motivates the application of seismic sounding, which is explained in section 2.2.5.

2.2.1. Magnetics

Magnetic anomaly maps display the spatial variations of the Earth's magnetic field, which are caused by spatial variations of the magnetisation of soil and embedded objects. On the one hand, the magnetic field anomaly of a cavity depends on the magnetisation of the surrounding soil because void space as such is not magnetised. For example, a cavity in non-magnetic limestone would not be magnetically detectable at all, whereas a cavity in volcanic rock would be. On the other hand, the strength of an anomaly depends on the ratio of cavity diameter to depth. The instrumental resolution is of the order of 0.01 to 1 nT depending on the type of magnetometer. Figure 2 a shows the corresponding detection swell and its variation with soil type (red, black and blue lines in fig. 2 a). We find as a rule of thumb that a cavity can be detected if its top is not deeper than its diameter. However, the practical magnetic detection swell of a cavity may be much higher than the instrumental resolution under field conditions due to magnetic ›noise‹. The detection swell may rise to tens of nT or more depending on anthropogenic and natural magnetic objects scattered between the Earth's surface and the target, such as boulders, sherds or remains of younger buildings. In many cases this implies that cavities need to be much shallower than their diameter to be detectable by magnetics. Exceptions to this rule of thumb are cases where grave chambers are constructed from magnetic rocks. In these cases the magnetic field of the rocks overprints the magnetic anomaly of the void. Compared to the anomaly created by a void space, the resulting anomaly may be anything: weaker, zero or even much stronger and reversed in polarity, depending on the magnetisation strength of the rocks from which the chamber is constructed.

2.2.2. Gravimetry

The local mass or density deficit constituting a cavity causes a local minimum in the Earth's gravitational field. Therefore, micro-gravimetry is an established classical method for locating shallow hollows. Since gravimeters are very sensitive to ground motion the method is mainly applicable in low-noise environments such as the interior of churches. Pašteka and co-workers[7] provided a recent review of micro-gravimetric methodology and its application in archaeological prospection. Under field conditions modern micro-gravimeters show an instrumental resolution on the order of 5 to 10 µGal[8]. Test computations (fig. 2 b) show that the corresponding theoretical gravimetric detection swell is slightly more favourable than the magnetic one. This is because the gravitational anomaly decay rate is $1/r^2$, where r is distance from a sample mass, whereas the magnetic field anomaly decay rate is $1/r^3$. The gradient of the magnetic field, which is typically measured in archaeological prospecting, decays at $1/r^4$. In practice, however, the same rule of thumb applies to gravimetry as to magnetics, namely that the top of a cavity must not be deeper than its diameter to be detectable.

2.2.3. Electric Resistivity Tomography

Since empty space is a perfect electric isolator, cavities can be detected in principle by geoelectric measurements if the surrounding soil is at least a little electrically conducting. This would be the case in most soils except, for example, in extremely dry sand or limestone. Under field conditions geoelectric units are able to determine apparent electric ground resistivity with an accuracy of about 2 to 5 %[9]. Given this value it turns out that geoelectric prospection shows effectively the same detection swell for cavities as do magnetic and gravimetric measurements, namely that the depth of a cavity must not exceed its diameter to be detectable by ERT (fig. 2 c). This is primarily due to the fact that the spatial decay of the electric field disturbance follows the same distance law as magnetic field anomalies. Within this frame, howev-

7 Pašteka et al. 2020.
8 Pašteka et al. 2020.
9 E.g. Fediuk et al. 2020.

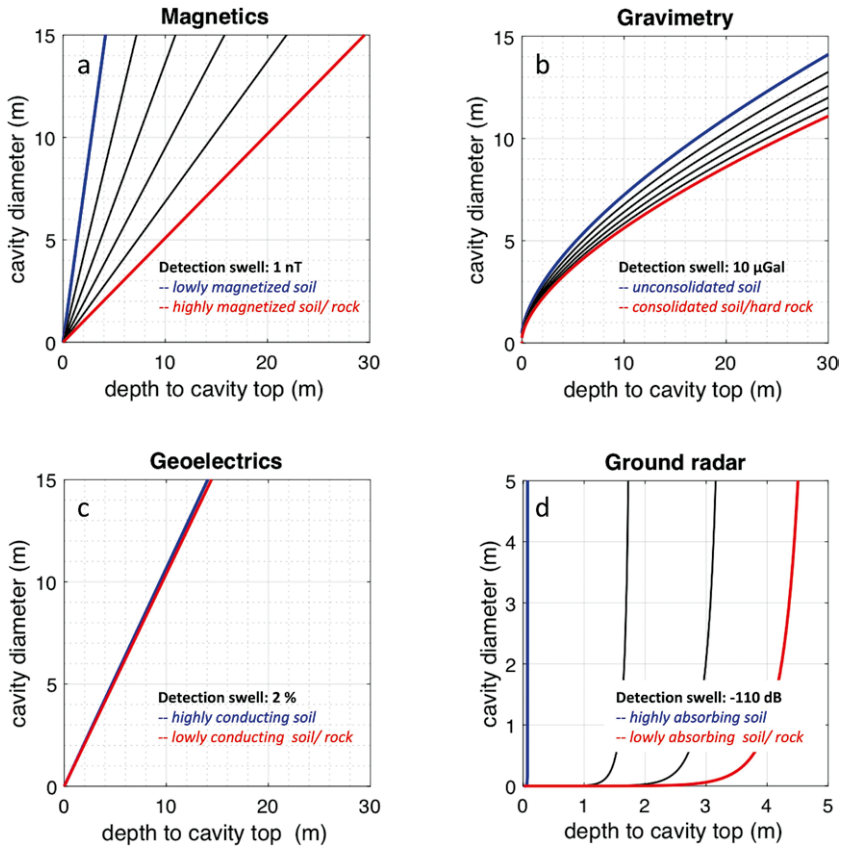

2 Detection thresholds for a cavity at varying depths expressed by the minimum diameter a cavity needs to have for being detectable by (a) magnetic single sensor, (b) gravimetric, (c) geoelectric and (d) GPR measurements (cf. fig. 3). Blue, black, red graphs are detection thresholds for different types of soil or rock in which the cavity is embedded. Assumed physical detection swells are given in the figures. Underlying equations and soil/rock parameters see Appendix A1

er, ERT measurements are more accurate in depth determination than magnetic or gravimetric measurements because electric sounding can be set up to reach predefined depth levels by increasing the distances between the electrodes. In contrast, magnetic and gravimetric measurements allow only the determination of a maximum depth if no further constraining information is available. However, in ERT an increasing sounding depth is always accompanied by a depth-proportional loss in spatial resolution.

Still, applying geoelectrics also for deeper levels can be helpful in assessing the bulk soil properties of major stratigraphic units in terms of electric resistivity, even if the spatial resolution is too low for detecting grave chambers. This is because the electric resistivity depends strongly on the porosity, moisture and clay content of the soil[10].

2.2.4. Ground Penetrating Radar

In contrast to magnetics, gravimetry and ERT, which rely on the analysis of quasi-static space-filling potential fields, GPR is based on electromagnetic wave propagation. Short, typically some 0.1 to 10 nanoseconds long, pulses of radar waves are transmitted into the ground and are reflected back to the Earth's surface from all structural interfaces, at which the dielectric permittivity, the electric conductivity or the magnetic permeability shows an abrupt, discontinuous change. The strength of the reflected signal received at the Earth's surface depends mainly on four quantities: the depth and size of the target, the reflection coefficient, which summarises the effects of the contrast of these material parameters across the interface, and the absorption of electromagnetic energy while the wave travels through the soil layers[11]. At

10 E. g. Kirsch 2009; Schön 2011.

11 E. g. Davis – Annan 1989.

the interface of a cavity the physical parameter contrasts are significant. Also, the cavity size is not a critical parameter since we consider metre-scale cavities. This is because the wavelengths of the commonly applied 100 to 800 MHz radar pulses are dm-scale thus creating Fresnel zones smaller than or similar to target size. Therefore, the critical factor limiting the detectability of grave constructions at greater depths is the radar wave absorption in the soils above the target (fig. 2 d). The typical dynamic range of commercial GPR recorders is about -96 to -110 dB[12], which defines a technical detection swell. Signals reflected from targets lying underneath this limit cannot be recognised as they fall below the instrument's sensitivity (fig. 3). The computations show that common GPR instruments can detect a metre-scale cavity up to a few metres' depth under typical soil conditions (fig. 2 d).

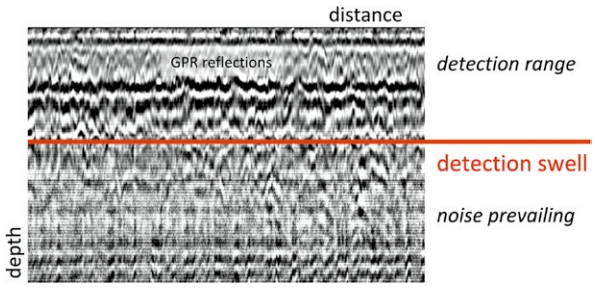

3 Example of detection range limitation of GPR records. The reflection image of a subsurface structure lying deeper than the detection swell cannot be detected because it is severely masked by electronic noise. The depth of the detection swell corresponds to the depths shown in fig. 2 d

2.2.5. Seismic Sounding

As an intermediate summary, it can be concluded that none of the geophysical methods commonly applied in archaeological prospecting can be expected to reliably detect metre-scale grave constructions at more than 10 m depth. The only method capable of reaching beyond this limit is seismic sounding. It has been developed since the 1920s for reservoir and scientific exploration of the Earth's crust at all depth levels. However, in archaeological prospection, seismics has been applied only sporadically, mainly for answering geoarchaeological questions[13]. Before turning to the question of structural resolution we shall provide some methodological background, especially with regard to the results presented by Meinecke et al. in this volume. More methodological details can be found in respective textbook articles[14].

Seismic exploration is based on the propagation of elastic waves inside the earth. Even with simple means like a sledge hammer it is possible to generate seismic waves that can travel several 10s of meters deep into the ground and back to the surface, enough for sounding most archaeological targets.

There are two types of seismic body waves: compressional and shear waves (P- and S-waves, respectively). In soils, their propagation velocities depend on substrate material, grain size, compaction and ambient pressure[15]. Therefore, the artificially generated seismic wave pulses travel through the subsurface with variable, soil-specific propagation velocity.

Seismic wave propagation in the subsurface is illustrated in Figure 4. It shows a numerical simulation of shear wave propagation in a model tumulus. The tumulus model (fig. 4 top left) consists of 2 layers (L1, L2) over a plane basement (B) and includes a grave chamber (C) at base level. Layers and basement differ in shear wave velocity (V_S) as a characteristic soil parameter. The chamber is assumed to be a cavity (V_S = 0 m/s). The *follow-up figures* show the computed shear wave propagation through the mound in the form of a series of ›snapshots‹[16]. At a stratigraphic interface or local obstacle one part of the wave energy is reflected or scattered back to the Earth's surface, thus forming a seismic echo (fig. 4, R1). The remaining

12 Davis – Annan 1989; Huang et al. 2007; Johansson 2009.

13 E. g. Stümpel – Rabbel – Schade 1988; Lütjen – Utecht 1991; Rabbel – Stuempel – Woelz 2004; Woelz – Rabbel – Müller 2009; Rabbel et al. 2014; Rabbel et al. 2015;.

14 E. g. Butler 2005; Rabbel 2010; Everett 2013.

15 E. g. Stümpel et al. 1984; Schön 2011.

16 Figure 4 illustrates many details of wave propagation, which we explain in this footnote for interested readers: T1 indicates the front of the wave transmitted directly from the source point through layer L1. After 50 ms it hits the interface between layers L2 and L1, where part of its energy is reflected back into L1 (wave R1) and part is transmitted into layer L2 (wave T2). Reflection R1 reaches the surface at 110 ms. While wave T2 moves along the top of layer L2 it radiates back continuously into the upper layer L1 creating wave T3 (110 ms et seq.). T3 reaches the surface again after some time. The downward travelling segment of wave T2 reaches the cavity at basement level at about 100 ms. Here it creates a strong wave R2 that is scattered back to the surface. The basement also creates a reflected wave (R3, see 130 ms), which is slightly delayed and much weaker compared to wave R2. The signal from the cavity (R2) reaches the surface at 190 ms travel time. Besides creating R2 and R3, the down-going part of wave T2 also radiates into the basement. The corresponding transmitted wave is indicated T4 (110 ms et seq.). While travelling along the top of basement B wave T4 radiates back into the upper layers, thus creating wave T5, which reaches the surface again after 190 ms. The transmitted (›refracted‹) waves T1 to T5 enable seismic refraction tomography. Waves R1 to R3 are reflections enabling seismic reflection imaging. Wave M1 (110 ms et seq.) results from a reflection of R1 at the Earth's surface.

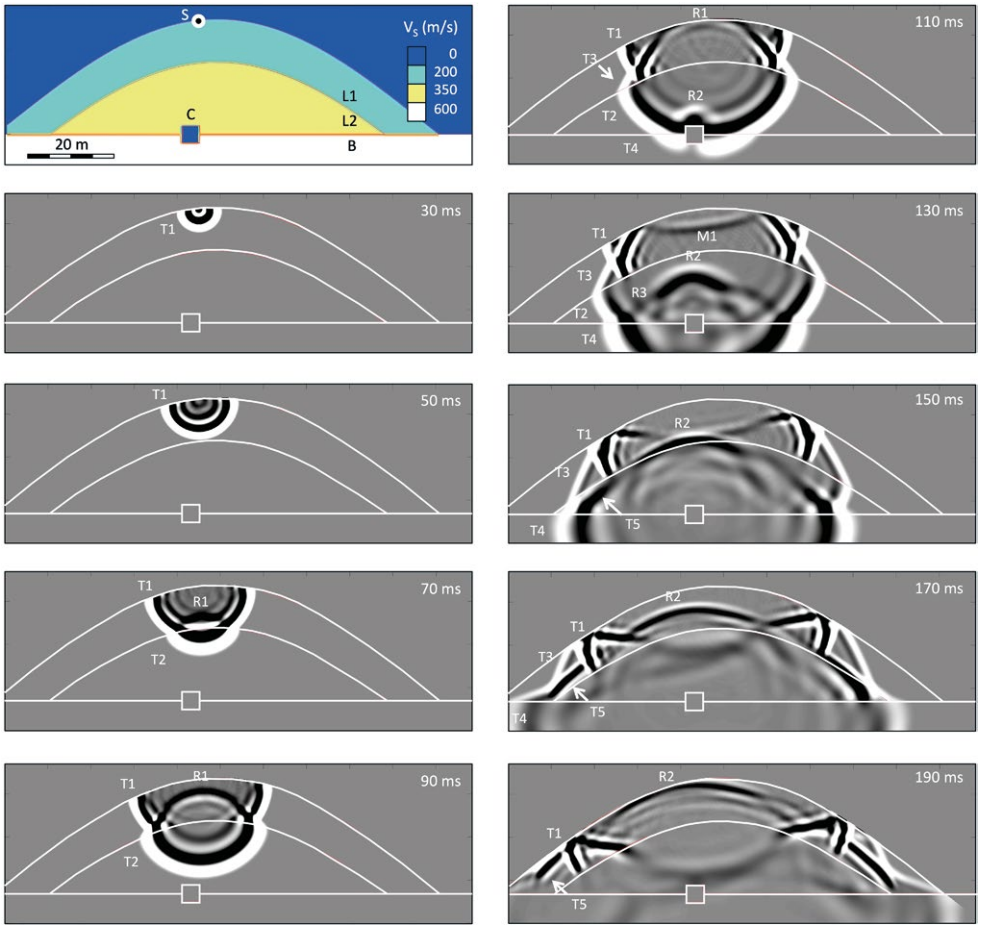

4 Numerical simulation of shear wave propagation in a tumulus. Top left: vertical section through a simple tumulus model (S: position of seismic signal source, L1, L2, B: layers; C: grave chamber; Vs: shear wave velocity). Follow-up figures: computed shear wave propagation in form of ›snapshots‹, i. e. wave motion frozen-in at the travel time indicated in the top right corner. Black & white are back & forth movement in the direction vertical to the drawing plane. R1 to R3: waves reflected from layer interfaces and grave chamber; T1: wave travelling through the top layer; T2 to T5: waves transmitted through internal layer interfaces; M1: wave reflected from the Earth's surface

part of the signal energy is transmitted into the deeper layers (fig. 4, T2. T4), from where part of the energy is again reflected back from the next interface and so on (fig. 4, R2. R3). Some portions of the transmitted wave are bent into travel paths parallel to the bedding plane if the velocity increases with depth. These ›refracted‹ waves will return to the Earth's surface, too, even without being reflected from an interface (fig. 4, T3. T5). Both reflected and refracted parts of the wave field are recorded with seismographs (›geophones‹) at the Earth's surface. The basic observables to be read from the seismograms are the arrival times and amplitudes (signal strengths) of the refracted and reflected waves.

To illuminate the targets at depth in a uniform way seismic energy pulses are fed into the ground at the Earth's surface at regularly spaced source points (›shot points‹), and the wave fields are recorded correspondingly by regularly spaced geophone arrays covering the investigation area along profile lines (fig. 5). In archaeological prospecting a typical source spacing is between one and a few metres, while geophone spacing is between 0.25 to 1 m depending on target depth and wavelength.

Seismic refraction and reflection arrivals contain different sorts of information. Accordingly, the approaches of data interpretation are somewhat different, too. Seismic refraction interpretation is basically an analysis of the arrival times of the refracted waves, which ›dive‹ through the stack of layers along bent travel paths and reach increasing depths with increasing path lengths (fig. 4, cf. ranges of T1, T3 and T5). According to Fermat's principle, the refracted waves are identified mainly as the very first arrivals in seismograms. With tomographic computations the arrival times are converted into depth sections of

5 Equipment for shear wave measurements: transmission of horizontal forces to the ground (left) and seismic recording line with 0.5 m spaced horizontal geophones (right)

P-wave or S-wave velocity, respectively, where stratigraphic layers can be identified as zones of similar seismic velocity (fig. 6, background colour). The bluish, greenish and brownish zones in Figure 6 indicate three construction phases of the mound evident from changes in shear wave velocity (Mecking et al. 2020).

In contrast, the digital processing of seismic reflection data offers the opportunity to create cross-sectional images of the subsurface in a more direct way. This is because the delay time, at which the echo returns to the Earth's surface, is related directly to the depth of the reflecting target. The final outcome of seismic reflection processing is a seismic reflection-depth section showing the amplitudes of the reflected waves plotted to scale at the correct horizontal and depth coordinates of the reflecting subsurface point (fig. 6, aligned black wiggles). Seismic reflection images delineate the contours of subsurface strata and obstacles. They are richer in structural detail than the tomographic velocity-depth sections based on refraction measurements. However, seismic reflection and refraction results need to be combined for obtaining optimum reliable structural images and characterising layers through their seismic velocity.

Using the whole wave field without discriminating reflection and refraction arrivals is the concept of an interpretation method called full-waveform inversion (FWI), which represents the current state of the art. The first applications to archaeological targets have been published[17], but the method is still under development. It requires super-computing facilities and, therefore, has not become a standard technique yet.

Returning to the goal of locating grave chambers it can be stated that cavities indeed represent a significant contrast in density and seismic velocity with respect to the surrounding soil that can be sensed in principle by both refracted and reflected seismic waves. However, refractions and reflections are different in resolution. Because of ›wave front healing‹ subsurface obstacles such as cavities need to have a

17 Dokter et al. 2017; Köhn et al. 2019; Schwardt et al. 2020.

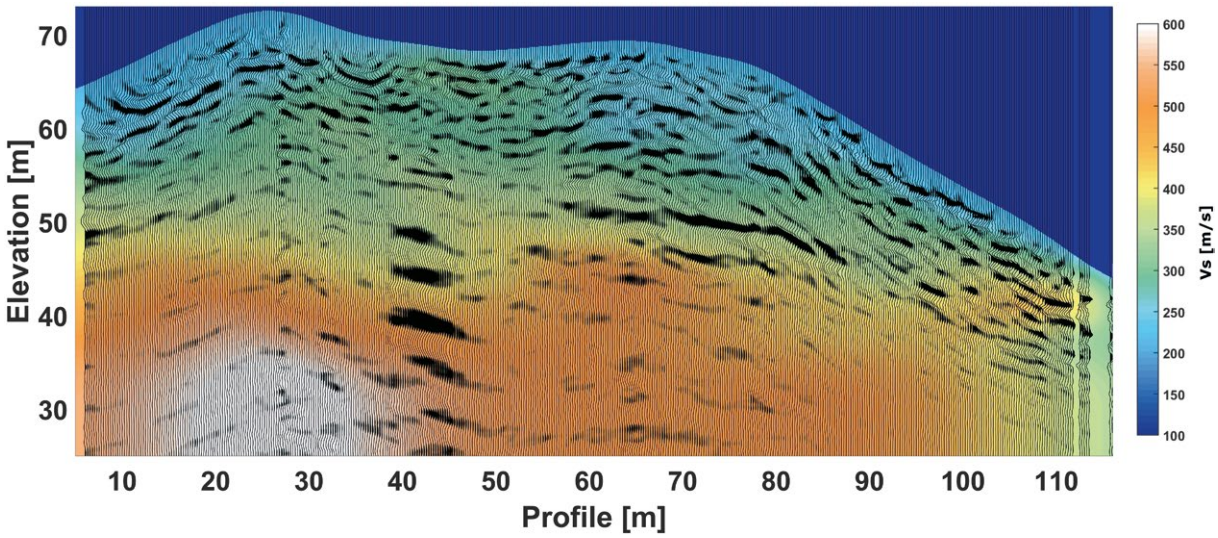

6 Example of combined seismic reflection and tomographic depth sections through Yığma Tepe (S-wave profile SH0, for location and details see Pirson et al. 2018 fig. 44 and Mecking et. al. 2020). The background colour shows shear wave velocity derived from seismic refraction tomography. Overlaid in black wiggles is the corresponding seismic reflection section

minimum size of the diameter of the 1st Fresnel zone to be locatable by means of refraction traveltime tomography[18]. This critical diameter increases with the square root of the depth of the obstacle and with wavelength (fig. 7, dot-dashed line). In contrast, the resolution limit of reflection seismic imaging is much less dependent on target depth (fig. 7, solid line). Under low ambient noise conditions it is theoretically of the order of a quarter of the dominant wavelength at target depth[19]. A more realistic estimate is half the dominant wavelength, as it is plotted in Figure 7. The increase of resolvable target diameter with depth in Figure 7 (solid line) is caused only by the depth increase of seismic velocity, which leads to an increase of wavelength as well. For typical near-surface soil conditions seismic wavelengths are on the order of metres, whereas the Fresnel zone diameter increases continuously to 10 m and more with increasing depth. For this reason, seismic refraction investigations are well suited for identifying major stratigraphic layers, but, for locating metre-scale grave constructions, seismic reflection measurements are to be preferred. Note that for depths greater than 8 to 10 m the theoretical resolution limit of seismic refraction is still somewhat better than the geoelectric resolution (fig. 7, cf. dashed and dot-dashed lines).

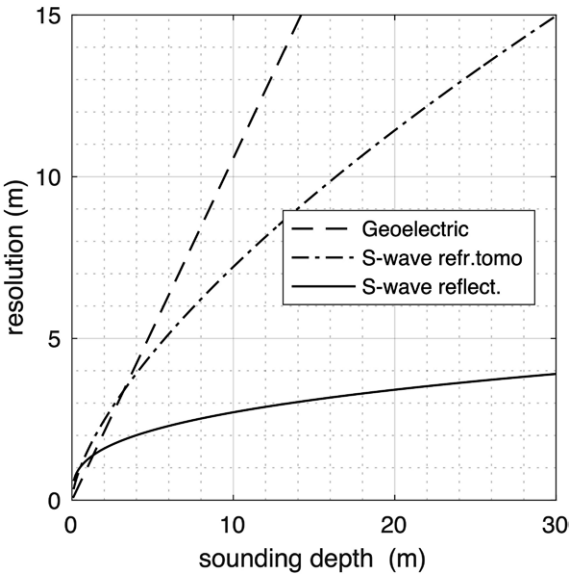

7 Minimum diameter a target needs to have for being identifiable through of shear wave reflection, shear wave refraction and geoelectric sounding (solid, dot-dashed, dashed lines, respectively). The seismic curves apply to a partially saturated sandy soil compacting with depth under its own load (see details of computation in Appendix A.2). The geoelectric curve is the same as in fig. 2

Still, metre-scale targets remain on the edge of detectability even for seismic reflections if they are located at greater depths or embedded in heterogeneous soils. Therefore, to increase spatial resolution as much as possible, the wavelength of the artificially generated seismic signals should be kept as short as possible. This can be achieved partly by the selection of the mechanical source type (sledge hammer, weight drop, electrodynamic vibrator) but only to a

18 Nolet – Dahlen 2000.

19 E. g. Yilmaz 2001, chapter 11.

certain extent, because the soil-specific absorption of energy in unconsolidated ground limits the affordable maximum signal frequencies typically to the order of 100 or 150 Hz. Wavelength is the ratio of wave velocity to frequency. In unconsolidated, partially saturated soils the velocities of S-waves are slower by a factor of 2 to 5 than the velocities of P-waves[20]. Therefore, S-waves typically show much shorter wavelengths than P-waves at comparable frequencies. For this reason, S-waves are to be preferred in principle for archaeological prospecting.

Technically, S-wave signals are generated with a horizontal point force, for example a hammer blow, applied at the source points located on the profile (fig. 5, left). The preferred force direction is oriented horizontally, orthogonal to the direction of the receiver line. In this way so-called SH-waves are generated, the movement of which occurs mainly in the horizontal plane.

However, the mechanical weakness of near-surface soils and the related tendency to shear slip often adversely affect the coupling of the applied horizontal forces to the ground and may practically restrict the range of S-waves to a few tens of metres only. Therefore, for sounding ranges of hundreds of metres, it is often necessary to use P-waves despite their larger wavelengths. P-waves are generated through vertical point forces, for example vertical hammer blows, which usually show excellent force-to-ground coupling. For this reason, sounding a monumental grave mound in its full horizontal and vertical extension will often require both P- and S-wave measurements.

2.3. Prospection Concept Summary

Reconsidering the exploration tasks defined for monumental grave mounds in section 2.1, the following intermediate conclusions can be drawn at this point:

1. *Grave chambers* can be assumed to be basically metre-scale cavities surrounded by soil. As a rule of thumb, they can be detected by potential field methods – magnetics, gravimetry and ERT – only if their horizontal and vertical diameters are not smaller that the depth of the top from the surface. If we consider, for example, a spherical cavity with a diameter of 5 m, this means that the bottom of the cavity must be no deeper than 10 m in order to remain locatable. Because of the strong absorption in partially saturated soils the detection limit of GPR lies mostly even shallower although the decimetre-scale spatial resolution of GPR is much better than the resolution of the other potential field methods. Seismic measurements can easily sound geological structures down to depths of tens of metres. However, their spatial resolution depends strongly on the producible wavelengths. For typical onshore field conditions seismic reflection measurements using horizontally polarized S-waves (SH-waves) are the most promising approach for locating metre-scale cavities. P-wave reflection seismics is suitable, too, but only if the signal frequencies that can be generated and received are higher by a factor of 2 to 5 when compared to the frequencies of S-waves.
2. *Stratigraphy*: The considerations outlined above for grave chambers and dromoi can be adapted to the question of stratigraphy almost directly. Magnetics and gravimetry do not need to be considered because they cannot resolve strata at all; at most, indications of horizontal contrasts may be found. GPR and ERT can be applied to determine near-surface layering with respective decimetre to metre-scale resolutions down to a few metres deep. For sounding deeper structures seismic reflection measurements should be applied in combination with refraction measurements. The combination is fruitful because refraction measurements provide more reliable seismic velocity information than reflection measurements, whereas reflection measurements show higher spatial resolution. Because of their superior spatial resolution, S-wave investigations are in principal preferable to P-wave investigations. However, P-waves still need to be considered as an alternative to overcome practical problems of force-to-ground coupling and range. This applies especially to transmitting signals horizontally through mounds at the base level.
3. *Near-surface archaeological targets*: Due to their near-surface position this sort of target can be investigated with the well-established archaeological prospection methods.

20 E. g. Stümpel et al. 1984; Schön 2011.

8 Yığma Tepe, instrument carrier for magnetic sensors lowered on a rope (Photo: W. Rabbel)

3. Realisation of Measurements

Beyond theoretical considerations on how to select the most promising prospection methods, the exploration of monumental tumuli may also require solutions to specific operational problems caused by steep slopes, slippery soils and rocks covering the surface. This became evident through the studies performed on Pergamon's Yığma Tepe[21]. Similar problems occurred in earlier studies, for example in the investigation of Nemrud Dağ as documented photographically by Lütjen and Utecht[22], though in a different geological setting.

Yığma Tepe is the largest tumulus of ancient Pergamon. It has a diameter of 158 m and a height of 32 m above ground level. Depending on erosion, the slopes show a variable dip from 20° to 35°, and in some places even more. The tumulus consists of alluvial sediments permeated with pebbles and boulders, partly forming patchy surface layers which are barely walkable without support.

Dealing with these conditions differs depending on whether the sensors need to be moved during profiling or whether they can be deployed in array form beforehand and then remain static during the measurement. The first case applies to ground radar and magnetics, the second to seismics and geoelectrics.

Deploying seismic and electric sensors (fig. 8a) along the slopes was time consuming but not connected with fundamental technical difficulties, because the helpers could crawl up the hill using a rope where necessary. Profiling gaps were unavoidable only in

21 For results see Meinecke et al. in part III of this volume; Mecking et al. 2020; Mecking et al. 2021.

22 Lütjen – Utecht 1991.

the steepest sections. However, with simple means, it was not possible to install advanced seismic signal generators, such as electrodynamic vibrator systems[23], on the slopes. Therefore, after some testing, the use of sledge hammer blows turned out to be the only feasible seismic source. Special care had to be taken to solidly couple the sensors in the loose surface soil. Electrodes had to be watered for electric coupling in the soil surface, which was otherwise too dry.

Most magnetic profiling was carried out with single sensors because the common sensor array-carrying carts were not usable along the slopes. On walkable sections a hand-held Overhauser gradiometer was used. For the steepest sections a special instrument carrier was constructed, which could be lowered from the top and lifted up again hanging on a rope. The carrier was equipped with two Cs-magnetometers and a GPS sensor for positioning (fig. 8b). During the single-sensor measurements a magnetic base station was run to correct external magnetic field variation.

Ground radar sounding was performed in two modes. Reconnaissance profiles extending along the whole slope could be realised only along a few example transects. Areal GPR measurements, which are usually archaeologically more informative, were applied on the top of the mound and at selected sites on the flanks, uphill of then ongoing excavations to virtually extend the unearthed structures. With standard equipment, GPR antennae were not useable on the mound's flanks. Therefore, a guide rail was constructed, along which an idler gear could be moved. The guide rail was anchored in the strike-line of the mound flank and the GPR antenna attached to the idler gear with a rope. By varying the length of the rope a set of parallel profiles of well-defined spacing could be realised, then the guide rail was moved and the procedure started again until the whole survey area was GPR-scanned.

With regard to the prospection targets listed in section 2.1 we wish to emphasise three aspects of field measurements, which proved to be helpful in excavation planning and geophysical interpretation:

1. Combining test excavations and geophysical sounding of the same near-surface key locations is of two-fold benefit. It enables the mutual optimising and guiding of excavation and prospection and provides ground truthing of geophysical subsurface structures (fig. 9). For example, at Yığma Tepe, ground truthing confirmed that high electric resistivity anomalies are most likely indicative of solid rock enrichment in the surrounding soil.
2. For sounding depths greater than 5 to 10 m geoelectrical measurements lose significantly in resolution. However, in combination with S-wave reflection imaging, ERT may still help to constrain the material of subsurface objects causing observed seismic reflections. This is illustrated by an example from Yığma Tepe (fig. 10): Whereas a seismic structure is identifiable at all depth levels, the resolution of ERT decays significantly at depths > 10 m. However, the electric tomography still suggests that the complex structure at upper right is a soil volume heavily enriched with boulders.
3. The same applies to seismic refraction measurement providing the subsurface distribution of seismic wave velocities. The geometry of stratigraphic structures can be determined much more accurately from seismic reflection images than from seismic velocity tomograms (fig. 6). However seismic refraction tomography is extremely helpful in identifying the variation of soil types and their compaction states[24].

23 Polom et al. 2013.

24 A detailed discussion can be found in Mecking et al. 2020.

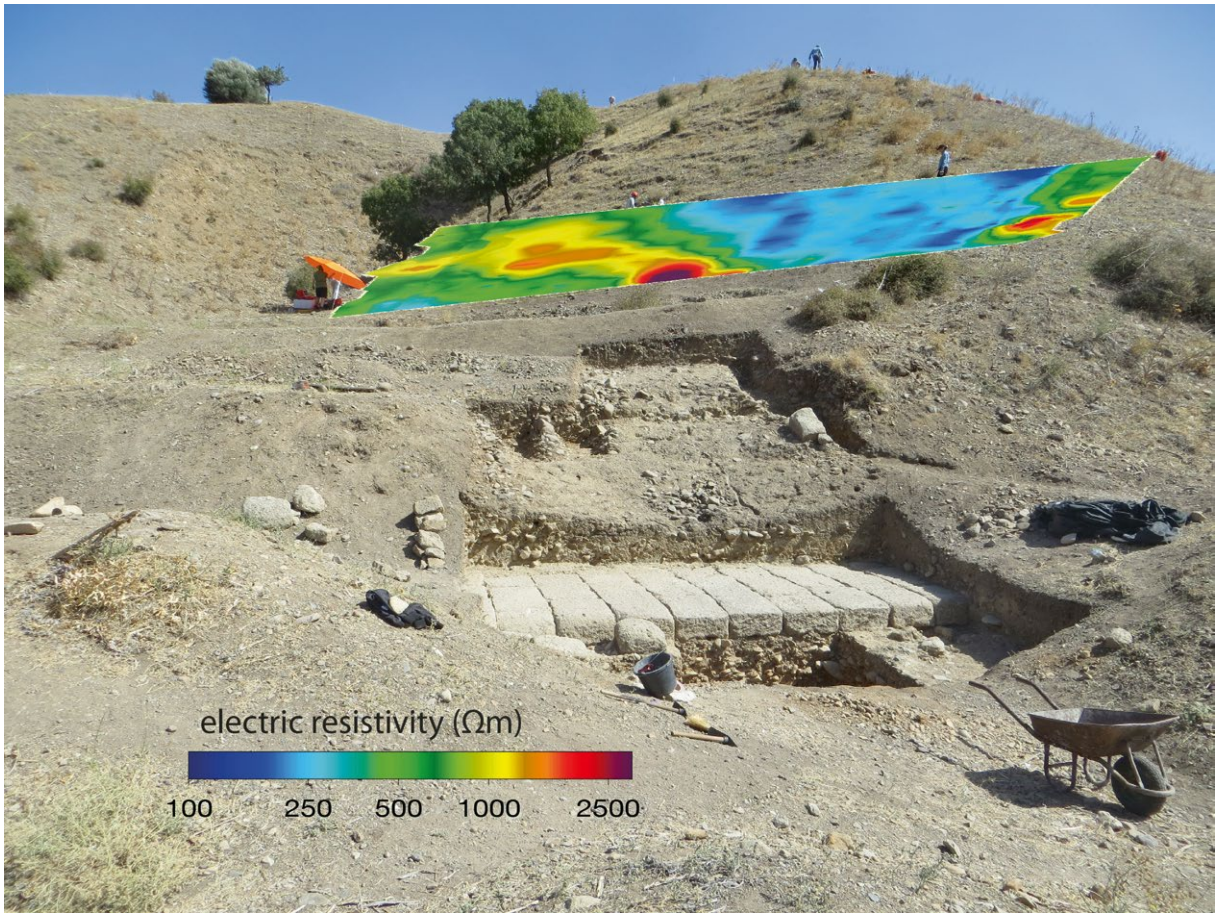

9 Geoelectric measurements applied to virtually extend an archaeological sondage at Yığma Tepe (Sondage PE17/So 05, cf. Pirson et al. 2018, figs. 35–38) upslope. High electric resistivity anomalies are indicative of solid rock enrichment

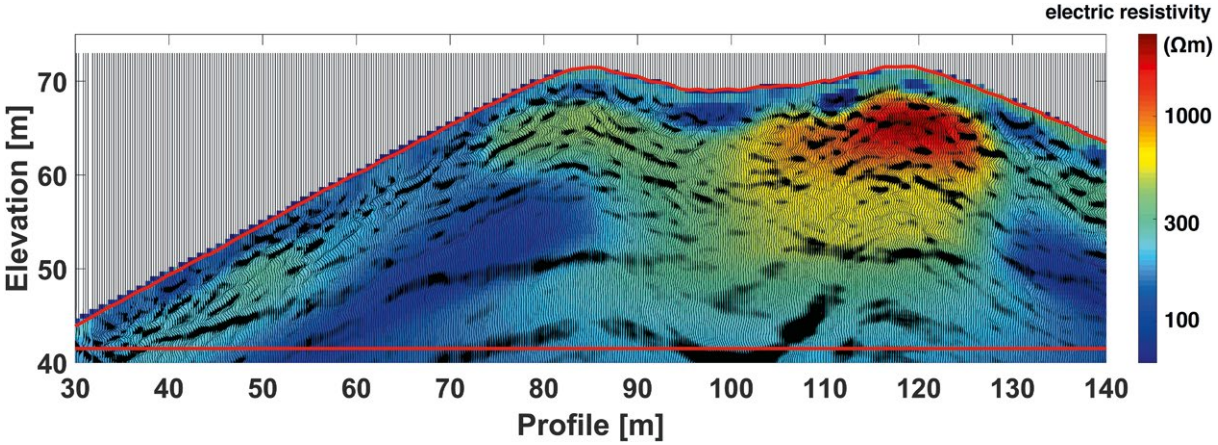

10 Example of combined S-wave reflection imaging and electric resistivity tomography at Yığma Tepe (location and further details see Pirson et al. 2018, fig. 44 seismic profile OW12, and Pirson et al. 2019, fig. 28 ERT profiles P2-P6-P3). The background colour is electric resistivity, black filled wiggles show reflecting internal interfaces

4. Conclusions

In exploring monumental grave mounds, three groups of targets and related geophysical approaches can be distinguished depending on the size and depths of the targets and on the sounding depth and resolution of the applied methods.

Grave chambers and dromoi can be understood as voids with typical horizontal and vertical diameters of a few metres. They are mostly impossible to detect with standard methods of archaeological prospecting (i. e., magnetics, geoelectrics and ground radar) if they are located deeper than about 10 m. Instead, the application of seismic reflection, especially shear wave seismic, is the most promising approach, because sounding depths of several tens of metres at metre-scale resolution can be achieved even with standard equipment.

Stratigraphy: The layering of monumental mounds, which may represent different construction phases and levels of varying soil compaction and moisture contents, can best be explored by applying a combination of seismic reflection, seismic refraction and electric resistivity tomography. In this approach, the layer boundaries are most reliably determined by seismic reflection, whereas seismic P- and S-wave velocities and electric resistivity values serve as attributes to characterise the soil type, moisture content and degree of compaction of the layers.

Near-surface archaeological targets are understood as targets at depths of only a few metres, including remains of ritual architecture, constructional elements or evidence of secondary usage. These can be investigated with all standard methods of archaeological prospection. We recommend combining geophysical measurements with targeted test excavations as it allows the optimising of excavation activity and the ground truthing of geophysical findings at the same time.

Acknowledgements

In this context we wish to thank the Geophysical Instrument Pool of the Deutsches Geoforschungszentrum Potsdam (GIPP), Umweltforschungszentrum Leipzig (UFZ), the University of Hamburg and the University of Karlsruhe for lending us geophysical equipment.

Appendix

A.1 Detection-Depth Limits of Cavities for Magnetic, Gravimetric, Geoelectric and Ground Radar Measurements

For computing the detection-depth limits of grave chambers shown in Figure 2 we approximate the hypothetical chambers using spherical cavities. This assumption maximises the material contrast to the surrounding soil giving the computation the character of an optimistic estimate. Regarding gravimetric and magnetic measurements, this single assumption was made because the additional assumption of walls surrounding the void would – with one exception – increase the average density and magnetisation of the chamber fill and decrease the difference of this value in regard the surrounding matrix. The exception is a hypothetical chamber constructed from volcanic rocks showing a very high magnetisation, much higher than the surrounding soil; in this case the magnetic signal could be higher than estimated and the detection-depth limit improved. For the geoelectric measurements the addition of walls to the model cavity would have no significant effect on the detection limit because the empty space is a perfect isolator and creates maximum resistivity contrast in both cases. Also, for GPR measurements adding walls to the model would not significantly change the strength of the reflected signal because the maximum reflection coefficient is associated with the free surface of the cavity anyway.

The formulae for the detection-depth limits can be derived from general expressions of the geophysical signal strength that exists in analytical form for spherical inclusions in an otherwise homogeneous half-space (references given below). To obtain the detection-depth limit one has to identify the respective signal strength variable with the signal detection threshold, which is the minimum signal strength resolvable in field measurements. Then the equations are rearranged to give the cavity radius as a function of cavity centre depth for given detection threshold and physical soil parameters.

In the corresponding *equations (1) to (4)* given below the variable r_{min} is the minimum radius the cavity needs to have to be detectable if its centre is at depth h_0. The top of the cavity is then located at depth $z_{top} = h_0 - r_{min}$. The definitions of the remaining variables and the range of values applied for the diagrams in Figure 2 are listed below each equation.

For determining the *magnetic detection threshold*, we assumed that the measurements be performed with a single-sensor instrument recording the total intensity. We do not consider gradiometers, which are usually applied in archaeological prospecting, because they are designed to be most sensitive for structures located in the uppermost few metres only. From the underlying formula of the magnetic total field anomaly of a spherical inclusion[25] with contrasting magnetic susceptibility we obtain the minimum radius r_{min}^{magn} the inclusion needs to have for being detectable with magnetic total field measurements if the top of the cavity is at depth h_0:

$$r_{min}^{magn} = \left(\Delta T_D \frac{3}{2B_0 |\Delta k|}\right)^{1/3} h_0 \qquad (1)$$

with the following variables and values for the graph in Figure 2a:

Variable	Meaning	Unit	Values (fig. 2a)	Comment
ΔT_D	Magnetic detection threshold	nT	1	Magn. background ›noise‹
B_0	Ambient magnetic field	nT	45000	Regional value for Turkey
Δk	Magnetic susceptibility contrast	10^{-5} SI	12.5 25, 50, 100, 200 400	Soil (low Fe content) ... soil (high Fe content)

25 E. g. Blakely 1995, 93 f.

The *gravimetric detection threshold* is derived from the corresponding formula of the gravimetric anomaly of a spherical inclusion with contrasting density[26]. We obtain the minimum radius r_{min}^{grav} the inclusion needs to have for being detectable with gravity field measurements if the top of the cavity is at depth h_0:

$$r_{min}^{grav} = \left(\Delta g_D \frac{3}{4\pi G|\Delta\rho|} h_0^2\right)^{1/3} \quad (2)$$

with the following variables and values for the graph in fig. 2b:

Variable	Meaning	Unit	Values (fig. 2b)	Comment
Δg_D	Gravimetric detection threshold	µGal	10	2× instrumental resolution
G	Gravitation constant	$m^3/(kg\ s^2)$	$6.67*10^{-11}$	
$\Delta\rho$	Density	kg/m^3	1400	Subsoil
			1650, 1900, 2150, 2400	...
			2650	Hard rock

For determining the *geoelectric detection threshold* we assumed a Schlumberger electrode configuration with electrode distance larger than the target depth. From the corresponding formula of the electric field anomaly[27] caused by a spherical inclusion with contrasting specific electric resistivity we obtain the minimum radius r_{min}^{elec} the inclusion needs to have for being detectable with geoelectric measurements if the top of the cavity is at depth h_0:

$$r_{min}^{elec} = \lim_{\rho_1 \to \infty} \left(\Delta M_D \frac{\rho_0 + 2\rho_1}{|\rho_0 - \rho_1|}\right)^{\frac{1}{3}} h_0 \approx 1.25\, \Delta M_0^{1/3} h_0 \quad (3)$$

Here, the middle term (without »lim«) applies to any resistivity contrast, whereas the right term applies to a cavity. The variable and values for the graph in Figure 2c are:

Variable	Meaning	Unit	Values (fig. 2c)	Comment
ΔM_D	Electric detection threshold	–	0.02	Instrumental accuracy
ρ_0	Electric resistivity of half-space	Ωm	$<\infty$	
ρ_1	Electric resistivity of sphere	Ωm	∞	Empty space

An expression for the *GPR detection threshold* can be obtained by combining the effect of absorption as described in the so-called radar equation[28] with an equation describing explicitly the effect of curved interfaces on reflection strength[29]. We obtain the minimum radius r_{min}^{GPR} the inclusion needs to have for being detectable with GPR measurements if the top of the cavity is at depth h_0:

$$r_{min}^{GPR} = \left(\Delta P_D e^{-2\alpha z_{top}} \frac{R}{2z_{top}} - 1\right)^{-1} z_{top} \quad (4)$$

with the following variables and values for the graph in Figure. 2d:

Variable	Meaning	Unit	Values (fig. 2d)	Comment
ΔP_D	GPR detection threshold	dB	–110	Typical system performance
R	Reflection coefficient	–	1	Maximum possible value
α	Absorption coefficient	dB/m	20	Wet clay
			5, 2	...
			0.2	Dry sand

Under laboratory conditions the signal detection threshold would be something like two-times the instrumental noise level; under field conditions it is typically two-times the ›ambient noise‹ level. For getting a realistic estimate one has to consider that the ›ambient noise‹ not only includes technical effects of the instruments and their handling but also environmental effects and a sort of ›apparent noise‹ resulting from random subsurface heterogeneity. This ›apparent noise‹ is actually a part of the subsurface response and usually correctly recorded in a technical sense. However, it

26 E. g. Blakely 1995, 51 f.
27 Töpfer 1969, 199. 211 f.
28 E. g. Davis – Annan 1989, 536 f.
29 Hilterman 1975, 748. 760 f.

may still mask the signal of the cavity. Irregularly distributed sherds, stones or even rubbish may cause background random heterogeneity. Its level is clearly variable from place to place and difficult to estimate reliably before a measurement has taken place.

One aspect that is not considered in the applied formulae is the shape of the geophysical field anomaly. This concerns especially magnetic, gravimetric and electric measurements whereas GPR is not seriously affected. As a rule of thumb, the half-width of the geophysical field anomalies as observed at the Earth's surface is approximately equal to the centre depth of the cavity. This means, for example, that the main part of a field anomaly created by a cavity at 15 m depth will extend over an area of 30 × 30 m at the mound surface and that a multiple of this area has to be mapped to enable this long-wavelength signal to be distinguished from the geological background. If the related amplitudes are close to the detection limit, this may be a difficult task. So, also from this perspective, the detection limits of magnetics, gravimetry and geoelectrics given in Figure 2 have to be regarded as an optimistic estimate.

A.2 Resolution of Seismic Reflection and Refraction Measurements

The resolution of seismic measurements can be described through the time delay between two successive seismic signals that is necessary to recognise them as two separate events. The spatial equivalent of this time delay is the 1st Fresnel zone. This is the subsurface volume hosting those points whose scattered signals contribute to a considered arrival by constructive interference according to Huygens' principle. The reflections of two objects located within this Fresnel volume are barely distinguishable if at all.

Under optimal conditions seismic reflection images have a theoretical resolution limit of a quarter wavelength (so-called λ/4 criterion), which corresponds to a time separation of a quarter period (T/4) between two successive signals[30]. Here λ = vT where v is the seismic wave velocity at the depth of the reflecting interface. This maximum resolution can only be achieved if the digital processing includes a so-called migration process, which virtually shifts the observation plane from the Earth's surface to the depths of the reflections.

»Optimal conditions« means that the signal shape is sharp, the signal-to-noise ratio high and the subsurface is »simple« in the sense that it does not contain too many reflecting or scattering interfaces arranged in a complex manner. Since this is rarely the case, it is more realistic is to assume λ/2 or T/2 as the resolution limit. This can be verified by considering the distances between well-locatable arrivals in Figures 6 and 10 (λ/2 corresponds to the length of a »half-oscillation« filled-in black). For computing the corresponding resolution limit of seismic reflections (Figure 7, solid line) we used the equation

$$d_{min}^{refl} = v\,(h_0)\,T/2 \tag{5}$$

where d_{min}^{refl} can be understood as the minimum distance of two objects to be distinguishable from each other, and $v(h_0)$ is seismic velocity at depth h_0. For the graph in Figure 7 we used the following S-wave velocity-depth function typical for dry sand[31]:

$$v\,(h_0) = 127\,h_0^{0.33} \tag{6}$$

where units are m/s and m, respectively. It agrees qualitatively with the S-wave velocity values determined by Mecking et al.[32] for Yığma Tepe; T is the effective period of recorded reflections, here set to a typical value of 0.02 s (corresponding to 50 Hz).

Compared to migrated seismic reflection images the resolution of seismic refraction tomography is significantly worse. For computing the graphs shown in Figure 7 we applied the following equation[33] of Nolet – Dahlen (2000):

$$r_{min}^{refr} = [\lambda x_0/\pi]^{1/2} = [\tilde{v}\,(x_0)\,Th_0/\pi]^{1/2} \tag{7}$$

r_{min}^{refr} is the minimum radius that a seismic velocity anomaly in principal needs to exceed to be locatable by seismic traveltime tomography. x_0 and $\tilde{v}\,(x_0)$ are distance and average seismic velocity between receiver location and the anomaly centre; T is again the main signal period. For $x_0 = h_0$, the average velocity can be obtained from equation (6) by depth-integrating the root-mean-square formula giving $\tilde{v}\,(h_0) = v\,(h_0)/1.33$.

30 E. g. Yilmaz 2001, chapter 11; Rabbel 2010.
31 Schön 2011.
32 Mecking et al. 2021.
33 Nolet – Dahlen 2000.

In principle, seismic refraction measurements are able to provide significantly higher resolution than estimated through equation (7). Achieving this would require considering not only first arrival traveltimes but the whole scattered wavefield and applying a »full-waveform inversion« (FWI). This method is currently under development. As it requires high-performance computing facilities it cannot be regarded as a standard method although the first successful applications of FWI to archaeological targets have been presented recently[34].

Abstract

Tumuli are major components of ancient land- and cityscapes, with the more monumental examples reaching tens of metres in height. Investigating their interior is a challenging task because archaeological excavations are usually restricted to the surface layers, and conclusions by analogy drawn from other, known, mounds are problematic because no general regularities of construction have been found so far. From a geophysical perspective the investigation of monumental grave mounds consists in locating and classifying possible metre-scale archaeological objects at up to tens of metres' depth. This causes a significant resolution and range problem for most of the sounding methods typically applied in archaeological prospecting. In the present article we analyse the capabilities of geophysical prospection methods in detecting grave chambers in the interior of monumental tumuli by determining method-specific detection limits of cavities. These thresholds represent the minimum size of a cavity for being locatable as a function of depth, instrument sensitivity and measurement conditions. Based on this review we develop a prospection concept that includes three groups of targets: (1) *Grave chambers and dromoi*, understood as voids with typical diameters of a few metres: These cannot be detected with magnetics, geoelectrics or ground radar if their depths are greater than 10 m as an order of magnitude. The most promising method is shear wave (S-wave) reflection seismic, which enables sounding depths of several tens of metres at metre-scale resolution. (2) *Stratigraphy*: Layered construction phases of tumuli and internal levels of varying soil compaction and moisture contents can be identified and classified in terms of seismic wave velocity (both compressional [P-] and S-wave velocities) and electric ground resistivity. These can be reliably derived from a combination of reflection seismic, seismic refraction tomography and electric resistivity tomography. (3) *Near-surface archaeological targets* down to depths of a few metres, such as remains of ritual architecture and secondary usage, can be investigated with all standard methods of archaeological prospection. Generally we recommend combining geophysical measurements with targeted test excavations to optimise excavations and ground-truth geophysical findings.

Keywords: Archaeological prospection, geophysics, dectection limits, grave chambers, dromoi

Illustration Credits

Figs. 1–10 Institute of Geosciences – Applied Geophysics, Kiel University, Kiel, Germany

34 Dokter et al. 2017; Köhn et al. 2019; Schwardt et al. 2020.